

Original Article
Infectious Disease



Evaluation of host and bacterial gene modulation during *Lawsonia intracellularis* infection in immunocompetent C57BL/6 mouse model

Perumalraja Kirthika , Sungwoo Park , Vijayakumar Jawalagatti ,
John Hwa Lee *

College of Veterinary Medicine, Jeonbuk National University, Iksan 54596, Korea

 OPEN ACCESS

Received: Oct 20, 2021

Revised: Jan 2, 2022

Accepted: Jan 27, 2022

Published online: Feb 26, 2022

*Corresponding author:

John Hwa Lee

College of Veterinary Medicine, Jeonbuk National University, 79 Gobong-ro, Iksan 54596, Korea.

Email: johnhlee@jbnu.ac.kr

https://orcid.org/0000-0002-2028-2207

ABSTRACT

Background: Proliferative enteritis caused by *Lawsonia intracellularis* undermines the economic stability of the swine industry worldwide. The development of cost-effective animal models to study the pathophysiology of the disease will help develop strategies to counter this bacterium.

Objectives: This study focused on establishing a model of gastrointestinal (GI) infection of *L. intracellularis* in C57BL/6 mice to evaluate the disease progression and lesions of proliferative enteropathy (PE) in murine GI tissue.

Methods: We assessed the murine mucosal and cell-mediated immune responses generated in response to inoculation with *L. intracellularis*.

Results: The mice developed characteristic lesions of the disease and shed *L. intracellularis* in the feces following oral inoculation with 5×10^7 bacteria. An increase in *L. intracellularis* 16S rRNA and *groEL* copies in the intestine of infected mice indicated intestinal dissemination of the bacteria. The C57BL/6 mice appeared capable of modulating humoral and cell-mediated immune responses to *L. intracellularis* infection. Notably, the expression of genes for the vitamin B12 receptor and for secreted and membrane-bound mucins were downregulated in *L. intracellularis*-infected mice. Furthermore, *L. intracellularis* colonization of the mouse intestine was confirmed by the immunohistochemistry and western blot analyses.

Conclusions: This is the first study demonstrating the contributions of bacterial chaperonin and host nutrient genes to PE using an immunocompetent mouse model. This mouse infection model may serve as a platform from which to study *L. intracellularis* infection and develop potential vaccination and therapeutic strategies to treat PE.

Keywords: Animal model; mouse; mucin; immune response; cytokines

INTRODUCTION

Proliferative enteropathy (PE) is an intestinal disease with a wide host range [1-3], and is commonly diagnosed in pigs [4,5]. The bacterium responsible for PE multiplies in the cytoplasm of immature enterocytes, predominantly within those of the ileum and colon

ORCID iDs

Perumalraja Kirthika
<https://orcid.org/0000-0002-9638-1615>
 Sungwoo Park
<https://orcid.org/0000-0001-6309-1104>
 Vijayakumar Jawalagatti
<https://orcid.org/0000-0001-8492-5550>
 John Hwa Lee
<https://orcid.org/0000-0002-2028-2207>

Author Contributions

Conceptualization: Lee JH; Funding acquisition: Lee JH; Investigation: Kirthika P, Park S, Jawalagatti V; Methodology: Kirthika P, Park S; Resources: Lee JH; Supervision: Lee JH; Writing - original draft: Kirthika P, Jawalagatti V; Writing - review & editing: Kirthika P, Jawalagatti V, Lee JH.

Conflict of Interest

The authors declare no conflicts of interest.

Funding

This research was supported by Basic Science Research Program through the National Research Foundation of Korea (NRF) funded by the Ministry of Education (2019R1A6A1A03033084).

[6,7]. In horses, PE has been classified as an emerging disease as this disease has remained largely unaddressed [8]. *Lawsonia intracellularis* is thought to be transmitted by the fecal-oral route. After the successful entry into the intestinal lumen, *L. intracellularis* exhibit tropism for epithelial cell crypts, where they preferentially invade rapidly dividing immature enterocytes [9]. The gross pathological lesions of PE are often restricted to the intestinal epithelium and the distribution of active infection in other organs is yet to be elucidated. In infected pigs, *L. intracellularis* antigens have been detected in mesenteric lymph nodes, tonsillar crypt cells, and the peripheral circulation; these findings have been attributed to the distribution of bacterial antigens by infected macrophages [10,11]. The economic impact of PE on the swine and equine industries is the result of prolonged recovery and/or severely reduced growth performance of infected animals [12].

The pathogenesis of PE has been studied after challenging experimental pigs and foals using *L. intracellularis* isolates grown *in vitro* [13] or mouse enteroids [14]. There have been only a few studies reporting successful *L. intracellularis* infection of laboratory rodents and chickens, and the infection produced different disease outcomes [15]; however, hamsters have been reported to be both naturally and experimentally infected with *L. intracellularis*. Infected hamsters manifest profound weight loss with severe hyperplasia of the ileum, a syndrome similar to that observed in pigs [16]. Therefore, the hamster is used as an animal model of PE following infection with ileal homogenates harvested from naturally diseased pigs or with bacteria grown in pure cell culture.

The use of experimentally challenged pigs and foals to study PE increases the cost of research by manifold. Thus, we urgently need animal models of PE that are cost-effective and allow the analysis of the critical aspects of *L. intracellularis* infection, multiplication, pathogenesis, and transmission, and more importantly, support therapeutic testing and identification of vaccine candidates. Mice are the most commonly used animal models in research due to their small size, short reproduction time, high fecundity, and low maintenance cost [17]. Although INF- γ is shown to be required for intestinal epithelial hyperplasia in knockout mice infected with *L. intracellularis*, data regarding host-bacterial interactions in immunocompetent mice are limited.

In the current study, we evaluated the ability of *L. intracellularis* to infect immunocompetent C57BL/6 mice. The outcomes of this study may provide a better understanding of host-pathogen interactions in the C57BL/6 mouse model. To the best of our knowledge, there have been no previous studies of the ability of *L. intracellularis* to infect immunocompetent mice and compromise the intestinal barrier.

MATERIALS AND METHODS

Mice and ethics statement

Seven-week-old female specific-pathogen-free C57BL/6 mice (n = 50) were procured from Koatech Laboratory Animals, Inc. (Korea). All animal experiments were approved by the Jeonbuk National University Animal Ethics Committee (CBNU2015-00085). Animals were provided antibiotic-free deionized water and fed *ad libitum*. The mice were assigned to either the test (n = 30) or the control (n = 20) group.

Bacterial strain and experimental infection

The test group mice were experimentally infected with about 5×10^7 *L. intracellularis* (Enterisol Ileitis; Boehringer Ingelheim, Germany) administered by gavage. The control group received phosphate-buffered saline (PBS). For 5 consecutive weeks, the mice were weighed and their feces were collected. Blood samples were collected once weekly and stored at -20°C . Additionally, the ileum and spleen ($n = 5/\text{group}$) were collected for further analyses. The ileal tissue was processed for quantification of the *L. intracellularis* 16S rRNA gene. Further, the expression of genes encoding for mucin, pro- and anti-inflammatory cytokines, the vitamin B12 transporter and *Lawsonia* chaperonin *GroEL*. The spleen was processed for profiling of the T-cell population.

Evaluation of *L. intracellularis*-specific genomic DNA

DNA was extracted from feces with Exgene Stool DNA Mini Kit (GeneAll Biotechnology, Korea), following the manufacturer's instructions. The *L. intracellularis* 16S rRNA gene was amplified using the primers listed in **Table 1**. The PCR mixture was calibrated using a known number of *L. intracellularis* and performed as described elsewhere [18]. A negative result was assigned if no amplification ensued or for a threshold cycle greater than 36. The reactions were performed in triplicate for each sample.

Table 1. The primers used in this study

Gene	Primer sequence	Reference
16S rRNA	FP: 5'-GCGCGCGTAGGTGTTA-3' RP: 5'-ATGCTTGTTGTATTCTCT-3'	This study
<i>GroEL</i> (<i>Hsp60</i>)	FP: 5'-ACTAAGCGACATTACAAGCC-3' RP: 5'-CAAACCTCATTCTCAACCAC-3'	This study
Cubilin (intrinsic factor cobalamin receptor)	FP: 5'-CCGTGTTCTATTCTCAG-3' RP: 5'-ATGCTTGTTGTATTCTCT-3'	This study
Mucin 2	FP: 5'-GCTGACGAGTGGTGGTGAATG-3' RP: 5'-GATGAGGTGGCAGACAGGAGAC-3'	This study
Mucin 5AC	FP: 5'-CACACACAACCACTCAACC-3' RP: 5'-TCACACTTCAACCCTGAC-3'	This study
Mucin 1	FP: 5'-GCAGTCCTCAGTGGCACCTC-3' RP: 5'-CACCGTGGGCTACTGGAGAG-3'	This study
Mucin 4	FP: 5'-AACCTCAAACCACCACAAC-3' RP: 5'-TGTGTGCTCCTGAGTCTACTG-3'	This study
Mucin 12	FP: 5'-TCATCACCATAGAAAACCCAG-3' RP: 5'-GTCACACCCCAATAAGCAAG-3'	This study
Mucin 13	FP: 5'-CGGGAACAGGAAGTGTGAAG-3' RP: 5'-CAGCAAGATGAGGATGAGGG-3'	This study
IL-2	FP: 5'-CCTGAGCAGGATGGAGAATTACA-3' RP: 5'-TCCAGAACATGCCCGCAGAG-3'	[18]
TNF- α	FP: 5'-CATCTTCTCAAAATTCGAGTGACAA-3' RP: 5'-TGGGAGTAGACAAGGTACAACCC-3'	This study
IL-6	FP: 5'-GAGGATACCACTCCCAACAGACC-3' RP: 5'-AAGTGCATCATCGTTGTTTACATA-3'	This study
IFN- γ	FP: 5'-TCAAGTGCCATAGATGTGAAGAA-3' RP: 5'-TGGCTCTGCAGGATTTTCATG-3'	This study
IL-4	FP: 5'-ACAGGAGAAGGGACGCCAT-3' RP: 5'-GAAGCCCTACAGACGAGCTCA-3'	This study
CXCL1	FP: 5'-GCTTGAAGGTGTTGCCCTCAG-3' RP: 5'-AAGCCTCGCGACCATTCTTG-3'	[19]
IL-10	FP: 5'-GGTTGCCAAGCCTTATCGGA-3' RP: 5'-ACCTGCTCCACTGCCTTGCT-3'	This study
TGF- β	FP: 5'-CCGCATCTCCTGCTAATGTTG-3' RP: 5'-AATAGGCGGCATCAAAGC-3'	This study

FP, forward primer; RP, reverse primer.

Anti-*L. intracellularis* antibody

Antibody against *L. intracellularis* was developed in-house using the bacterial whole cell lysate (WCL). The antibody was raised in New Zealand white rabbit. Rabbit was injected subcutaneously with WCL mixed with equal quantity of Freund's complete adjuvant. A booster dose was administered 15 later using Freund's incomplete adjuvant. Two weeks post-booster, sera sample was collected from the rabbit and used in the subsequent experiments.

Western blot analysis

Total protein (20 µg) extracted from mouse ileal tissue was separated on a 10% sodium dodecyl sulfate polyacrylamide gel, transferred to 0.45 µm pore size nitrocellulose membranes (Bio-Rad, USA) The primary anti- *L. intracellularis* antibody at a dilution of 1:500 was used to detect the immunoreactivity. An horseradish peroxidase (HRP)-conjugated anti-rabbit-IgA antibody (1:6,000; Southern Biotech, USA) was used as secondary antibody. The membranes were developed with DAB substrate and images were documented.

Protein digestion and mass spectrometric analysis

The uppermost immunodominant band was excised from the gel and digested as previously described [19]. Briefly, the excised gels were destained in 30 mM potassium ferricyanide and 50 µL of 100 mM sodium thiosulfate, dehydrated with acetonitrile (ACN), and finally dried in a vacuum centrifuge for 30 min. The gels were reswollen with 5 µL of 25 mM ammonium bicarbonate containing 10 ng of trypsin at 4°C for 30 min and then digested overnight at 37°C. After tryptic digestion, peptides were extracted three times with 50% ACN containing 5% formic acid. The extracted solutions were pooled and lyophilized. The dried peptide was dissolved in 2 µL 0.1% (vol/vol) trifluoroacetic acid and used for matrix-assisted laser desorption ionization time-of-flight mass spectrometry (MALDI-TOF-MS) analyses. Mass spectra were prepared using an Ettan MALDI-TOF Pro mass spectrometer (GE Healthcare, USA).

Immunohistochemistry assay

The intestinal tissue samples collected and processed by Swiss rolling method followed by fixation for formalin fixation and paraffin embedding [20]. The sections were incubated overnight at 4°C with the primary anti-*L. intracellularis* antibody at a dilution of 1:500. The sections were then incubated for 1 h with HRP conjugated secondary antibody followed by 10 min with metal enhanced DAB substrate working solution. Percent positive area was quantified by Image J analysis (National Institutes of Health, USA).

Quantitative reverse transcription-polymerase chain reaction (qRT-PCR)

Expression of mucin, cytokine and virulence-associated gene transcripts in control and infected ileal tissues was measured using qRT-PCR [21]. The quantification of target genes was assessed relative to β-actin expression using the $2^{-\Delta\Delta CT}$ method [22]. The relative expression of the target genes was quantified and compared at each time point using the primers listed in **Table 1**.

Serological evaluation of the immune response

An enzyme-linked immunosorbent assay (ELISA) was employed to determine the *L. intracellularis*-specific IgA and IgG immunoglobulin response, as described previously [23]. Briefly, *L. intracellularis* bacteria were heated for 5 min at 95°C and centrifuged at 1.2×10^4 g for 60 sec. The supernatant was discarded and the pellet was resuspended in PBS. The wells of ELISA plates (Greiner, Germany) were coated with 100 µL of heat-killed *L. intracellularis* bacteria (4 mg/mL) in 100 mM sodium carbonate (pH 9.7). The *L. intracellularis*-specific IgA

was detected using serum from control and test mice and HRP-conjugated goat-anti-mouse antibodies (Southern Biotech) and measured using an automated ELISA spectrophotometer (Tecan, Austria) at 492 nm.

Flow cytometry immunophenotyping of T cell populations

Splenocytes harvested from the mice were analyzed for viability by diluting the samples in 0.4% trypan blue solution at a 1:1 ratio. Then, 3×10^6 cells per tube were stained for cell surface CD3, CD4, and CD8 markers using the following monoclonal antibodies: PE-labeled anti-CD3e, PerCPVio700-labeled anti-CD4, and FITC-labeled anti-CD8a (Miltenyi Biotec, Germany). Cells were gated on the basis of their forward and side scatter profiles.

Statistical analyses

The data are presented as the mean of the results obtained from 4 or 5 mice per group \pm standard deviations. The statistical analyses were performed using a two-tailed paired *t*-test for weight loss and an unpaired *t*-test for T cell responses and mRNA transcript expression in ileal tissue.

RESULTS

Assessment of an *in vivo* infection model using C57BL/6 mice

The average body weight of C57BL/6 mice administered 5×10^7 *L. intracellularis* by gavage was monitored and recorded compared to control mice receiving PBS. A weekly gain in body weight was recorded in the control group. In contrast, *L. intracellularis* infection experienced reduced weight gain in the infected group (Fig. 1A). Furthermore, to confirm *L. intracellularis* colonization of the intestine, the copy number of the *L. intracellularis*-specific 16S rRNA gene in feces was evaluated using quantitative PCR. The presence of *L. intracellularis* 16S rRNA gene copies in the ileal tissue of the infected mice (Fig. 1B) confirmed the ability of the bacteria to invade the host ileum. Furthermore, the infected mice were found to shed up to 50 *L. intracellularis* in feces on Day 3 post-infection, and by Day 15 post-infection up to 1,600 *L. intracellularis* 16S rRNA gene copies/g feces were recovered from the mice (Fig. 1C).

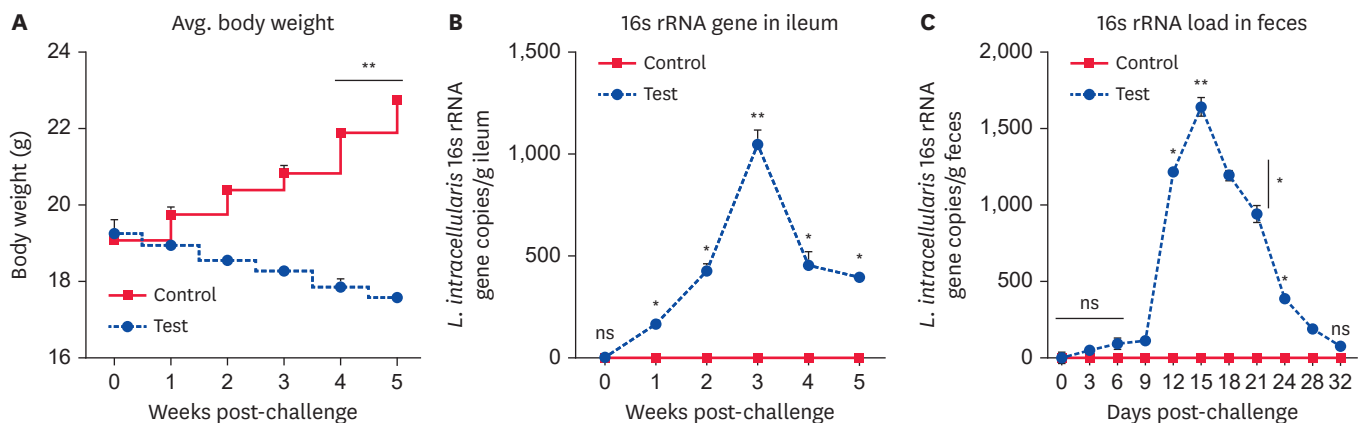


Fig. 1. Preliminary assessment of an *in vivo* *L. intracellularis* infection model in C57BL/6 mice. (A) The average body weight was recorded daily within 5 min of first contact for 4 or 5 mice per group. (B) Each week post-infection, mice ($n = 3$ /group) were sacrificed and the ileum was collected to evaluate the average number of *L. intracellularis* 16S rRNA genes per gram of ileal tissue. (C) The feces were collected from post-infection Day 0 up to Day 32. The data presented are quantitative polymerase chain reaction analyses of the average number of *L. intracellularis* 16S rRNA genes per gram of feces for 4 or 5 mice per group per day. The data represent one of two independent experiments.

ns, not significant.

Significant differences are depicted as follows: ^{ns} $p > 0.05$; * $p < 0.05$; ** $p < 0.01$.

Differential regulation of bacterial and host genes in the infected ileum

The expression of the genes for the *Lawsonia* heat shock protein 60 (*Hsp60*) and the host vitamin B12 receptor called *cubilin* was evaluated in ileal samples from infected mice; *Hsp60* expression revealed that *L. intracellularis* was successful in establishing infection in C57BL/6 mice intestine. A gradual increase in mRNA transcripts for the *Hsp60* was evident at 1 wk post-infection that continued up to 5 wk (Fig. 2A). After infection with *L. intracellularis*, the host *cubilin* gene was downregulated (Fig. 2B). Reduction of the vitamin B12 receptor may contribute to poor absorption of this essential vitamin during *L. intracellularis* infection. The Fig. 3 provides representative images of healthy control and diseased intestinal tissue with hemorrhagic congestion following *L. intracellularis* infection. Further, analysis of infected mouse intestine by H & E staining revealed crypt hyperplasia and damage to villi architecture (Fig. 3C and D).

Detection of *L. intracellularis* in ileal tissue by immunohistochemistry

The presence of *L. intracellularis* in paraffin-wax-embedded ileal tissue sections was detected using antibody specific for *L. intracellularis*. The immunohistochemistry assay demonstrated the presence of *L. intracellularis* bacteria in the apical cytoplasm of hyperplastic immature enterocytes (Fig. 4). Ileal sample isolated from mice at 1 wk post-infection revealed *L. intracellularis* localization. Greater immunoreactivity corresponding to *L. intracellularis* presence was observed in the ileal samples collected 2 and 3-wk post-infection.

Western blot analysis detected *L. intracellularis* proteins in the mouse intestine

To substantiate the presence of *L. intracellularis* in the intestines of infected mice, total proteins collected from the ileum of control and inoculated mice were separated on a polyacrylamide gel and blotted against *L. intracellularis*-antibody. Fig. 5A demonstrates the protein components of different molecular weights as determined using a wide-range Biofact marker kit. The antibody recognized three distinctive protein bands of *L. intracellularis*. The recognition of the proteins at approximately 25, 35, and 55 kDa was taken as a demonstration of *L. intracellularis* infection in the inoculated mice. Western blot analyses revealed that all mice receiving *L. intracellularis* expressed all three immunodominant proteins. The *L.*

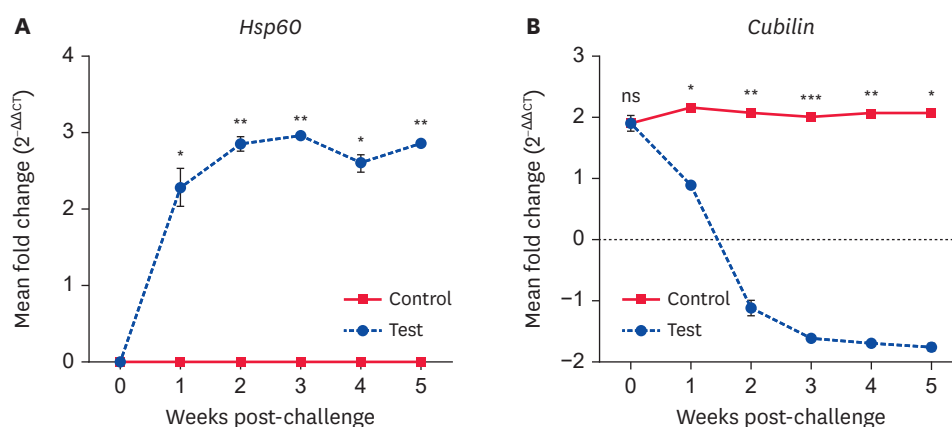


Fig. 2. Determination of bacterial and host gene expression in the ileum. Every week post-infection, mice ($n = 3/\text{group}$) were sacrificed and the ileum was collected to evaluate the expression of mRNA transcripts for (A) *GroEL* and (B) *cubilin* in the infected mice, and to compare the results with the outcomes in the control group. The data represent one of two independent experiments and are depicted as means \pm SE.

ns, not significant.

Significant differences are depicted as follows: ^{ns} $p > 0.05$; * $p < 0.05$; ** $p < 0.01$.

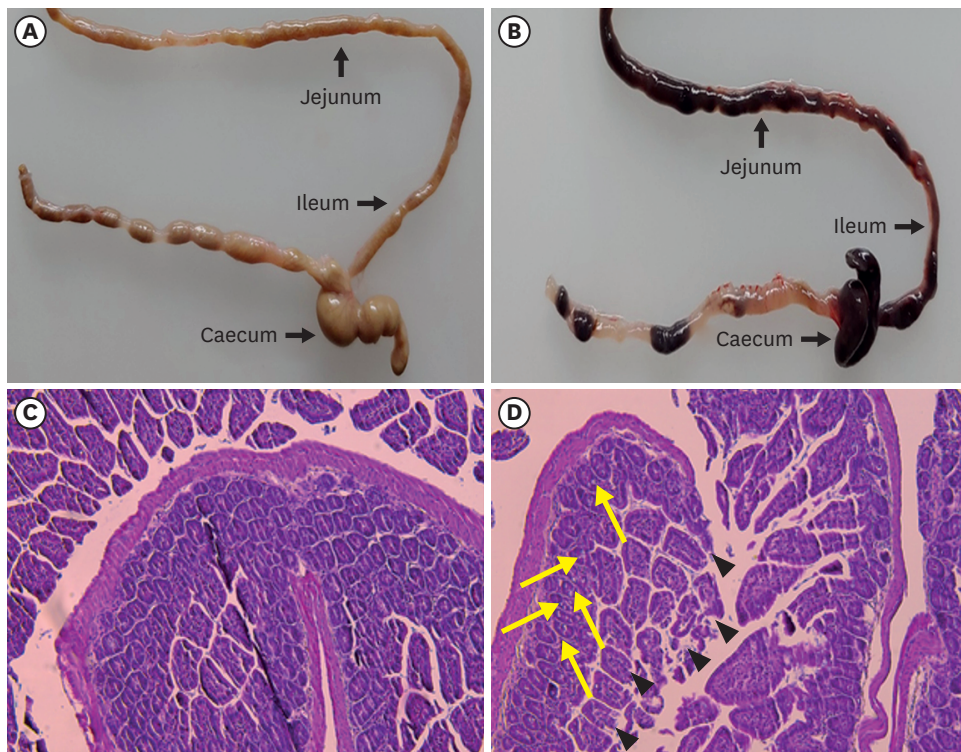


Fig. 3. The *L. intracellularis* infected intestine compared to the control. C57BL/6 mice infected with *L. intracellularis* causes hemorrhagic lesions throughout the intestine with pronounced damage to the caecum (B). The gross pathological lesions are shown in the representative image for *L. intracellularis* infected mice intestine (B) compared to the control (A). H & E stained intestinal tissue from control (C) and infected (D) mice have been shown. Note the crypt hyperplasia (yellow arrows) and loss of villi architecture (black arrowheads) in *L. intracellularis* infected mice intestine.

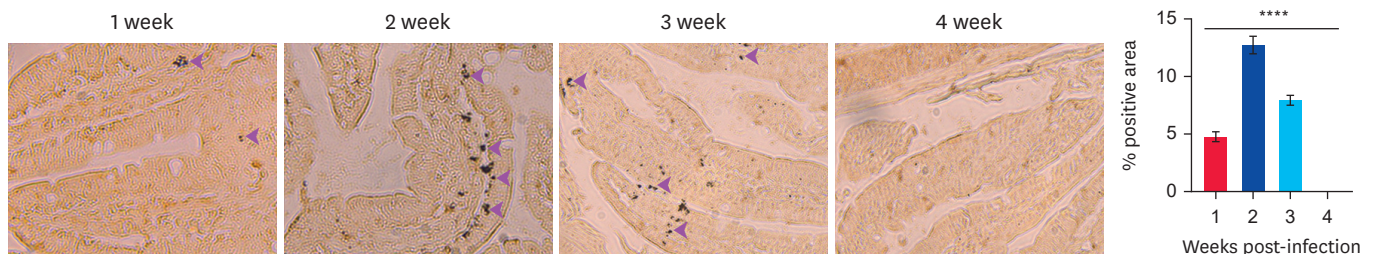


Fig. 4. Immunohistochemical staining of *L. intracellularis* in the ileum of 7-wk-old mice. The representative images demonstrate the *L. intracellularis* localization in the apical cytoplasm as visualized with peroxidase staining. The tissues were counterstained with methyl green. The ileal samples with dark brown positive staining (pink arrowheads) illustrate the presence of *L. intracellularis* in the tissue. Percent positive area from Image J analysis has been shown in the right panel as means \pm SE. The data representative of 5 mice per group from two independent experiments. Data was analyzed by analysis of variance with Tukey's multiple comparisons test. **** $p < 0.0001$.

intracellularis proteins were detected at 1 wk post-infection and remained detectable until 3 wk. The *L. intracellularis* proteins were not identified in control animals at any time point.

Identification of immunoreactive proteins

The immunoreactive protein bands were excised from the polyacrylamide gel by in-gel digestion (**Supplementary Fig. 1**) and identified using MALDI-TOF-MS based on peptide mass matching (**Supplementary Data 1**). A search of the NCBI database revealed that the protein, GroEL (was homologous with *L. intracellularis* Hsp60, a protein with a molecular mass of approximately 60 kDa (**Fig. 5B**; protein scores greater than 57 were considered significant, $p < 0.05$).

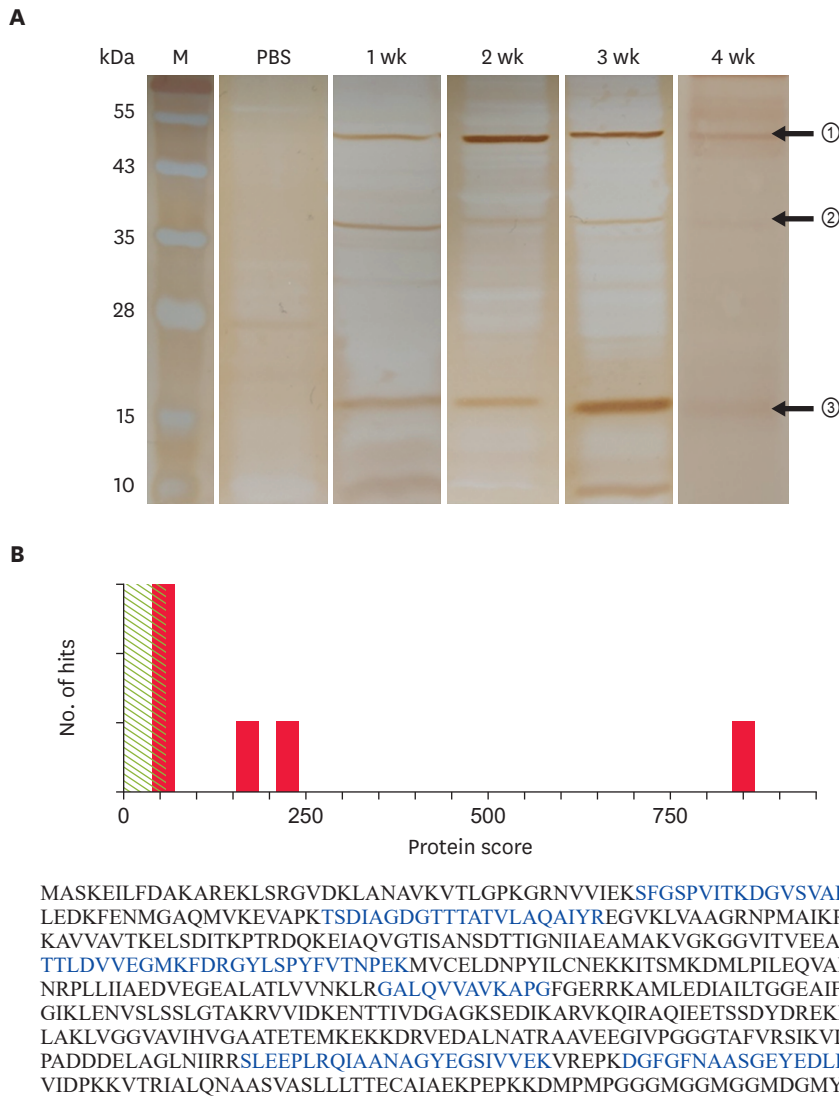


Fig. 5. Western blot and MALDI-TOF analyses of the *L. intracellularis* proteome. Protein samples were collected from the intestinal tissue of control and infected mice every week for 4 wk post-infection. (A) The presence of *L. intracellularis* in the intestinal tissue was confirmed by the identification of three immunoreactive bands at 25, 35 and 55 kDa. The representative images show positive immunoreactivity compared to the control group. (B) Identification results of immunodominant protein band. Protein scores ($n = 126$) that are greater than 57 are significant ($p < 0.05$). Protein scores were derived from ion scores on a non-probabilistic basis for ranking protein hits. The amino acid sequence of *GroEL* (a *Hsp60* homologue) has been presented with matched peptides depicted in bold. MALDI-TOF, matrix-assisted laser desorption ionization time-of-flight; M, molecular protein marker; PBS, phosphate-buffered saline.

Expression of mucin genes during *L. intracellularis* infection

The mRNA transcripts encoding secreted mucins 2 and 5AC, and membrane-bound mucins 1, 4, 12 and 13, in the ileum of healthy and inoculated mice, were measured using qRT-PCR (Fig. 6, $p < 0.05$). Upregulation of all the mucin genes was recorded for 2 wks post-infection. Interestingly, significant downregulation of the transcripts for secretory mucins was observed at 3 wk post-infection (Fig. 6). This downregulation may have been due to the increased number of invading bacteria within the enterocytes. On the other hand, the mRNA expression of membrane-bound mucins was upregulated for up to 5 wk post-infection (Fig. 6).

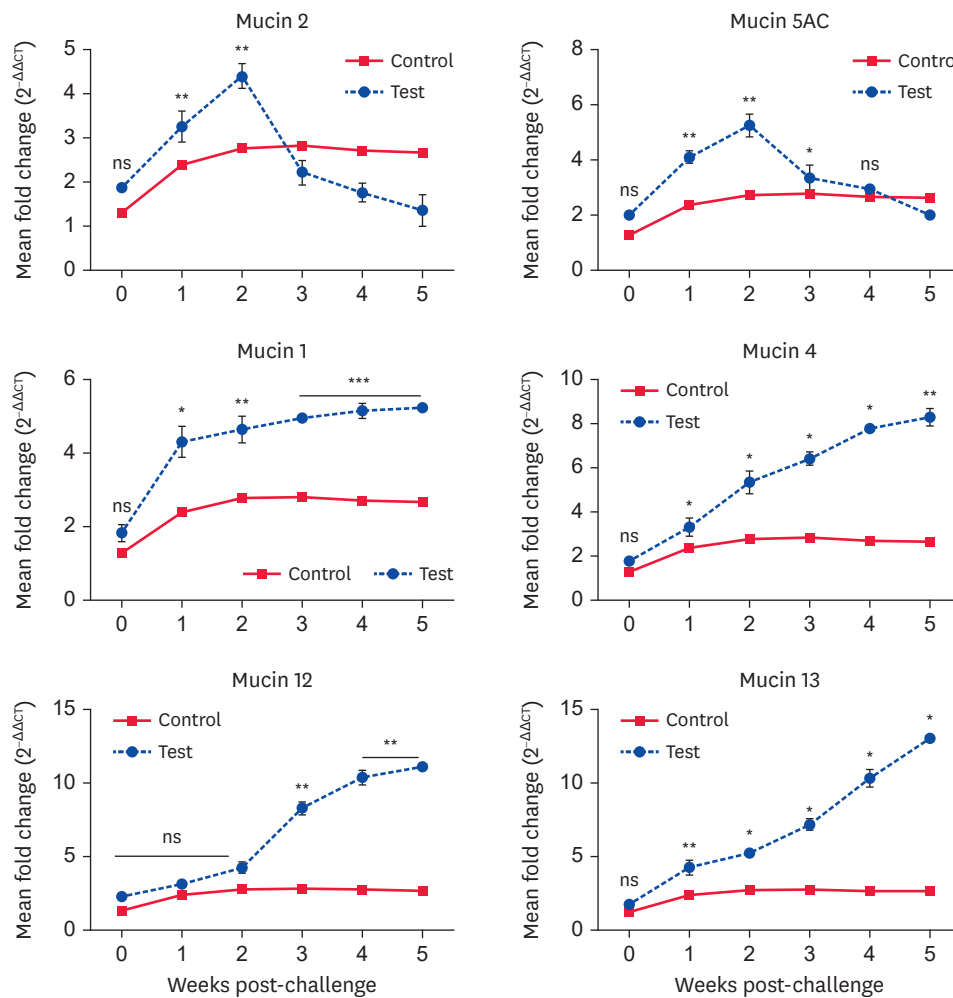


Fig. 6. Successful infection of the mice with *L. intracellularis* resulted in an altered mucin barrier. The mRNA levels of *muc1*, *muc2*, *muc4*, *muc5AC*, *muc12* and *muc13* in ileum of healthy mice and mice infected orally with *L. intracellularis* for 0, 1, 2, 3, 4 and 5 wk (n = 3 mice/group). Expression of mRNA encoding secreted and mRNA membrane-bound mucins (β -actin mRNA was used as an internal standard). The data represent one of two independent experiments and are depicted as means \pm SE. ns, not significant. Significant differences are depicted as follows: ^{ns}p > 0.05; * p < 0.05; ** p < 0.01; *** p < 0.001.

Antibody-mediated immune response

The *L. intracellularis*-specific IgA and IgG antibody levels within the serum were evaluated for 2 wk post-infection in the mice receiving the bacteria orally. The detection of circulating antibodies demonstrated the ability of *L. intracellularis* to elicit the B-cell mediated immune response in the infected mice. The production of IgA antibodies was greater than that of IgG (Fig. 7A).

Proliferation of CD4⁺ T-cells

Following infection with 5×10^7 bacteria, the splenocytes derived from the infected mice were subjected to flow cytometric analyses and the outcome was compared with the control group that received only PBS. The flow cytometric analyses showed an expansion of the T cell population (Fig. 7B) and a significant increase in the CD4⁺ subpopulation together with a reduction in the CD8⁺ T subpopulation.

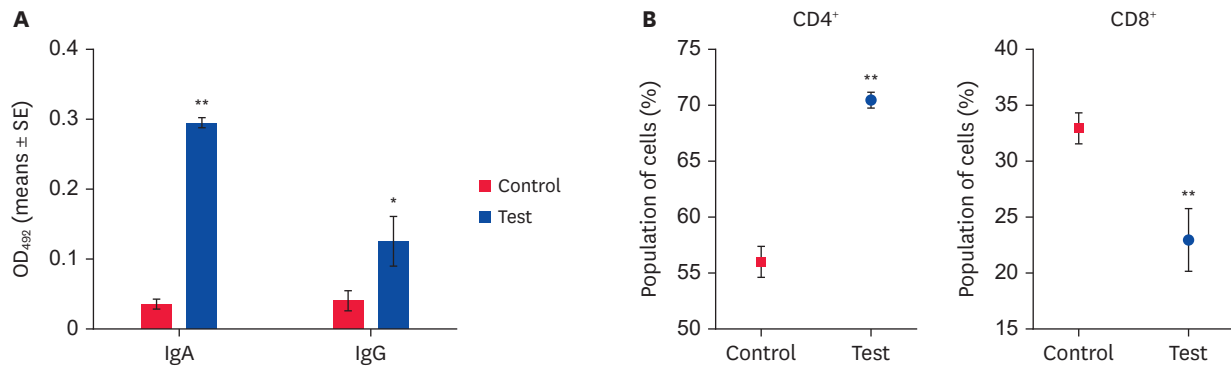


Fig. 7. Humoral and cell-mediated immune responses in infected mice. (A) Evaluation of induced IgA and IgG induction in mouse sera 2 wk post-infection with 5×10^7 *L. intracellularis*. The results are represented as the optical density at 492 nm (OD_{492}). The data represent one of two independent experiments and are depicted as means \pm SE for 4 mice per group. (B) T-cell proliferation was evaluated in freshly isolated splenocytes incubated with fluorochrome-conjugated antibodies against T-cell surface markers (PE-CD3, FITC-CD8 and PE-Cy7-CD4) and data collected for 10,000 cells per sample. The data are presented as the mean \pm SD percentage of splenocytes for 3 or 4 mice per group. The *p* values were determined using a two-tailed unpaired *t*-test. ns, not significant.

Significant differences are depicted as follows: **p* < 0.05; ***p* < 0.01.

Varied production of cytokines post-infection

The transcripts of pro-inflammatory cytokines IL-2, TNF- α , IL-6, and IFN- γ were upregulated at 7 d post-infection and continued to increase until the termination of the experiment at 5 wk post-infection (**Fig. 8**). The increase in the amount of transcript of pro-inflammatory cytokines appeared to be correlated with the degree of local inflammation and the severity of the enteritis [24,25]. In contrast, the expression of anti-inflammatory cytokines, including IL-4, IL-10, and TGF- β , increased at 4 wk post-infection (**Fig. 8**).

DISCUSSION

We established an experimental model of porcine *L. intracellularis* infection in immunocompetent C57BL/6 mice. The development of a mouse model is advantageous as it offers genetic and immunological tools to study the pathophysiology of PE in a cost-effective host. In this study, infection of seven-week-old immunocompetent C57BL/6 mice with *L. intracellularis* led to successful colonization of the intestine that caused severe weight loss (**Fig. 1A**). The invasion was confirmed by detection of *L. intracellularis* 16S rRNA gene copies in the ileal tissue and feces of the infected mice (**Fig. 1B and C**). Shedding of *L. intracellularis* bacteria along with significant loss of body weight from 7 d post-infection until the termination of the study indicated colonization of the intestine. The features of *L. intracellularis* infection in C57BL/6 mice were similar to those seen in porcine PE, wherein PCR detection of *L. intracellularis* in feces occurs from 2 to 38 d post-infection [26]. As a potential reservoir, mice may play a vital role in the epidemiology of PE [27]. In certain strains, such as ICR mice, the *L. intracellularis*-induced lesions were more severe than in other strains of mice [28]. Although extensive research has indicated *L. intracellularis* infection of mice occurs, there is limited information regarding the pathogenesis of infection, the interactions between bacterial and mouse tissues, or regarding the immune response during infection [15]. The upregulated expression of *L. intracellularis groEL* (**Fig. 2A**) in the ileum of infected mice indicated that *L. intracellularis* bacteria regulate the expression of chaperonin during the initial stages of colonization. GroEL (also known as *Hsp60*) is a stress response protein that promotes refolding and proper assembly of polypeptides and undergoes changes in cellular localization from cytosol to cell surface making it possible immunogen [29,30]. The upregulation of *groEL* expression was associated with the presence of multiple copies of the *L.*

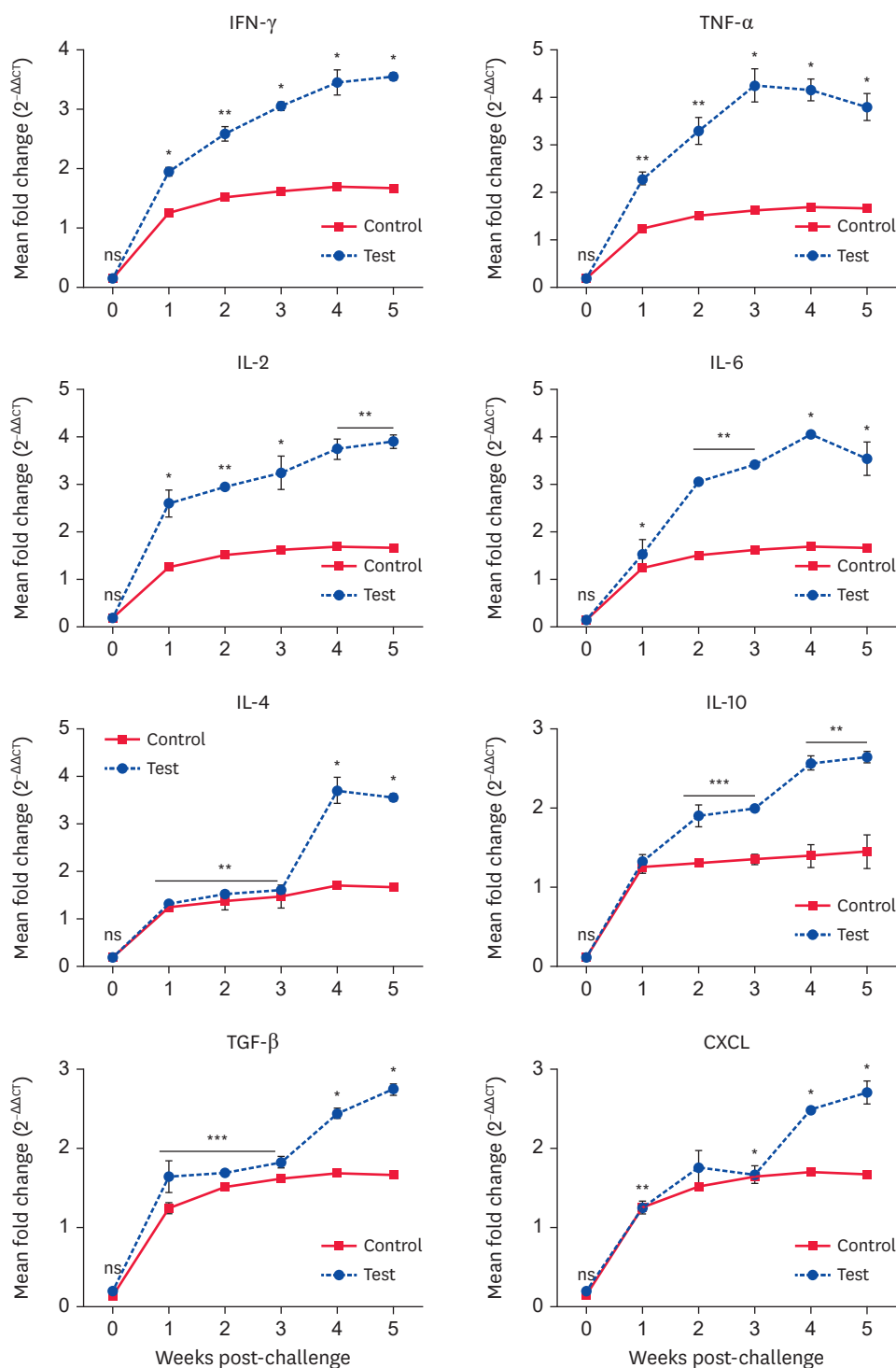


Fig. 8. Expression of pro-inflammatory cytokines in *L. intracellularis*-infected ileum. The Kinetics of cytokines mRNA expression in the ileal tissues of healthy and infected mice (n = 3 mice/group) was measured by semi-quantitative real time RT-PCR by using gene specific primers. β -actin mRNA was used as an internal standard. The data represent one of two independent experiments and are depicted as the means \pm SE. The p values were determined using an unpaired t-test. ns, not significant; RT-PCR, reverse transcription-polymerase chain reaction. Significant differences are depicted as follows: ^{ns}p > 0.05, *p < 0.05, **p < 0.01 and ***p < 0.001.

intracellularis 16S rRNA gene in the mouse ileum. Excessive bacterial colonization of the small intestine, including the ileum, leads to impaired absorption of vitamin B12 [31]. Downregulation

of the vitamin B12 receptor gene, *cubilin* in infected mice may have contributed to the severe weight loss due to malabsorption of vitamin B12 (**Fig. 2B**). The precise localization of *L. intracellularis* in ileum was confirmed using an immunohistochemistry assay (**Fig. 4**). The degree of positive immunoreactivity was consistent with the expression of *cubilin* mRNA. Additionally, western blot and MALDI-TOF analyses confirmed the presence of the *L. intracellularis* proteome in the ileal region of the small intestine (**Fig. 5**).

Bacteria using GroEL binds to host mucin to initiate colonization [30]. The pathogenic bacteria in the intestine are shown to alter the protective mucin barrier to enable better invasion and dissemination [32]. In this study, *L. intracellularis*-infection-mediated regulation of mucin genes was evident as early as at the first week post-infection. The mRNA expression of secreted mucins 2 and 5AC peaked at 2 wk post-infection (**Fig. 6**) as a result of an inflammatory response to the invading bacteria. Any insult to the epithelium causes upregulation of mucin genes and increased secretion of mucus to counter the pathogen [33]. Although expression of all the membrane-bound mucin genes (i.e., 1, 4, 12 and 13) continued to increase throughout the period of infection, significant downregulation of mucin 2 and 5AC was observed beginning at 3 wk post-infection. This downregulation of expression of the genes for secreted mucins may have been due to a specific inhibitory effect exerted by *L. intracellularis* [21]. In addition to hypersecretion of mucus, the host secretes immunoglobulins to inhibit pathogen invasion. Increased serum IgA and IgG in the infected mice two weeks post-infection was consistent with an *L. intracellularis*-specific acquired humoral immune response in the mice (**Fig. 7A**) [34]. The comparatively lower IgG titers revealed that the production of IgA was essential during *L. intracellularis* infection and IgG plays a minor role during the development of enteropathy [35]. Bacterial-infection-associated damage to the gut epithelium elicits a T-cell mediated immune response [36,37]. Here, the flow cytometry results suggested the cellular expansion was due to CD3⁺/CD4⁺ cells (**Fig. 7B**). The expansion of CD4⁺ cells is essential to induce early inflammatory responses in tissues and contributes to upregulation of cytokines (**Fig. 8**). The increased levels of TNF- α , IL-6 and IFN- γ in the infected mice suggested the potential for *L. intracellularis* bacteria to induce mucosal proliferation and necrosis. A similar response is seen in natural hosts during *L. intracellularis* infection, wherein acute intestinal hemorrhage or acute to chronic diarrhea with enterocyte hyperplasia are evident [38]. The upregulation of anti-inflammatory cytokines was observed during the later stages of the infection in the C57Bl/6 mice. Thus, tight regulation of the Th1- and Th2-mediated immune response against *L. intracellularis* seems crucial as it may determine the outcome of the disease. An increased Th1 response may lead to an acute form of the infection, whereas a predominantly Th2 response may lead to a chronic form of enteritis [5]. The ability of *L. intracellularis* to modulate the expression of its surface antigen may also influence the early stages of PE pathogenesis. The results of this study indicated *L. intracellularis* infection altered the expression of nutrient uptake genes, altered the intestinal protective barrier and elicited B- and T-cell mediated immune responses to cause the disease.

In conclusion, we showed that the C57BL/6 mice may serve as an *in vivo* model of infection to study *L. intracellularis* pathogenesis. The mice inoculated with the porcine variant of the bacteria showed signs of infection, and increased numbers of bacteria within ileal tissue and in the feces. The upregulation of *groEL* significantly contributed to the colonization of bacteria in the small intestine of infected mice. Bacterial proliferation in the small intestine caused downregulation of *cubilin* and altered the protective mucin barriers. Furthermore, the infection elicited B- and T- cell mediated immune responses in the host mice, contributing to inflammatory cytokine production. Overall, this study shows that the C57BL/6 mice

are susceptible to *L. intracellularis* infection and provides a plausible mechanism of the pathogenesis of PE. The successful establishment of *L. intracellularis* infection in mice provides a cost-effective system to continue investigation of the regulatory mechanisms involved in PE and to develop novel therapeutic targets to treat PE and the associated intestinal hyperplasia.

SUPPLEMENTARY MATERIALS

Supplementary Data 1

Raw data files generated from MALDI-TOF analysis of the protein sample.

[Click here to view](#)

Supplementary Fig. 1

SDS-PAGE of *L. intracellularis* protein lysate showing the excised protein band used in MALDI-TOF analysis.

[Click here to view](#)

REFERENCES

1. Cross RF, Smith CK, Parker CF. Terminal ileitis in lambs. *J Am Vet Med Assoc.* 1973;162(7):564-566.
[PUBMED](#)
2. Fox JG, Dewhirst FE, Fraser GJ, Paster BJ, Shames B, Murphy JC. Intracellular *Campylobacter*-like organism from ferrets and hamsters with proliferative bowel disease is a *Desulfovibrio* sp. *J Clin Microbiol.* 1994;32(5):1229-1237.
[PUBMED](#) | [CROSSREF](#)
3. Klein EC, Gebhart CJ, Duhamel GE. Fatal outbreaks of proliferative enteritis caused by *Lawsonia intracellularis* in young colony-raised rhesus macaques. *J Med Primatol.* 1999;28(1):11-18.
[PUBMED](#) | [CROSSREF](#)
4. Karuppanan AK, Opriessnig T. *Lawsonia intracellularis*: revisiting the disease ecology and control of this fastidious pathogen in pigs. *Front Vet Sci.* 2018;5:181.
[PUBMED](#) | [CROSSREF](#)
5. Vannucci FA, Gebhart CJ, McOrist S. Proliferative enteropathy. In: Zimmerman JJ, Karkiker LA, Ramirez A, Schwartz KJ, Stevenson GW, Zhang J. *Diseases of Swine*. Hoboken: John Wiley & Sons, Inc.; 2019, 898-911.
6. Guedes RM, Machuca MA, Quiroga MA, Pereira CE, Resende TP, Gebhart CJ. *Lawsonia intracellularis* in pigs: progression of lesions and involvement of apoptosis. *Vet Pathol.* 2017;54(4):620-628.
[PUBMED](#) | [CROSSREF](#)
7. Smith DG, Lawson GH. *Lawsonia intracellularis*: getting inside the pathogenesis of proliferative enteropathy. *Vet Microbiol.* 2001;82(4):331-345.
[PUBMED](#) | [CROSSREF](#)
8. Pusterla N, Gebhart CJ. Equine proliferative enteropathy--a review of recent developments. *Equine Vet J.* 2013;45(4):403-409.
[PUBMED](#) | [CROSSREF](#)
9. Huan YW, Bengtsson RJ, MacIntyre N, Guthrie J, Finlayson H, Smith SH, et al. *Lawsonia intracellularis* exploits β -catenin/Wnt and Notch signalling pathways during infection of intestinal crypt to alter cell homeostasis and promote cell proliferation. *PLoS One.* 2017;12(3):e0173782.
[PUBMED](#) | [CROSSREF](#)
10. Gebhart CJ, Guedes RM. *Lawsonia intracellularis*. In: Gyles CL, Prescott JF, Songer JG, Thoen CO. *Pathogenesis of Bacterial Infections in Animals*. 2010, 503-512.
11. Pereira CE, Resende TP, Armien AG, Laub RP, Vannucci FA, Santos RL, et al. Survival of *Lawsonia intracellularis* in porcine peripheral blood monocyte-derived macrophages. *PLoS One.* 2020;15(7):e0236887.
[PUBMED](#) | [CROSSREF](#)

12. Sampieri F, Vannucci FA, Allen AL, Pusterla N, Antonopoulos AJ, Ball KR, et al. Species-specificity of equine and porcine *Lawsonia intracellularis* isolates in laboratory animals. *Can J Vet Res* 2013;77(4):261-272.
[PUBMED](#)
13. Boutrup TS, Boesen HT, Boye M, Agerholm JS, Jensen TK. Early pathogenesis in porcine proliferative enteropathy caused by *Lawsonia intracellularis*. *J Comp Pathol*. 2010;143(2-3):101-109.
[PUBMED](#) | [CROSSREF](#)
14. Resende TP, Medida RL, Guo Y, Vannucci FA, Saqui-Salces M, Gebhart C. Evaluation of mouse enteroids as a model for *Lawsonia intracellularis* infection. *Vet Res*. 2019;50(1):57.
[PUBMED](#) | [CROSSREF](#)
15. Collins AM, Love RJ, Jasni S, McOrist S. Attempted infection of mice, rats and chickens by porcine strains of *Lawsonia intracellularis*. *Aust Vet J*. 1999;77(2):120-122.
[PUBMED](#) | [CROSSREF](#)
16. Cooper DM, Swanson DL, Barns SM, Gebhart CJ. Comparison of the 16S ribosomal DNA sequences from the intracellular agents of proliferative enteritis in a hamster, deer, and ostrich with the sequence of a porcine isolate of *Lawsonia intracellularis*. *Int J Syst Bacteriol*. 1997;47(3):635-639.
[PUBMED](#) | [CROSSREF](#)
17. Bryda EC. The Mighty Mouse: the impact of rodents on advances in biomedical research. *Mo Med*. 2013;110(3):207-211.
[PUBMED](#)
18. Nathues H, Holthaus K, grosse Beilage E. Quantification of *Lawsonia intracellularis* in porcine faeces by real-time PCR. *J Appl Microbiol*. 2009;107(6):2009-2016.
[PUBMED](#) | [CROSSREF](#)
19. Zhou M, Guo Y, Zhao J, Hu Q, Hu Y, Zhang A, et al. Identification and characterization of novel immunogenic outer membrane proteins of *Haemophilus parasuis* serovar 5. *Vaccine*. 2009;27(38):5271-5277.
[PUBMED](#) | [CROSSREF](#)
20. Bialkowska AB, Ghaleb AM, Nandan MO, Yang VW. Improved Swiss-rolling technique for intestinal tissue preparation for immunohistochemical and immunofluorescent analyses. *J Vis Exp*. 2016;113(113):54161.
[PUBMED](#) | [CROSSREF](#)
21. Bengtsson RJ, MacIntyre N, Guthrie J, Wilson AD, Finlayson H, Matika O, et al. *Lawsonia intracellularis* infection of intestinal crypt cells is associated with specific depletion of secreted MUC2 in goblet cells. *Vet Immunol Immunopathol*. 2015;168(1-2):61-67.
[PUBMED](#) | [CROSSREF](#)
22. Livak KJ, Schmittgen TD. Analysis of relative gene expression data using real-time quantitative PCR and the $2^{-\Delta\Delta C_T}$ Method. *Methods*. 2001;25(4):402-408.
[PUBMED](#) | [CROSSREF](#)
23. Richer L, Potula HH, Melo R, Vieira A, Gomes-Solecki M. Mouse model for sublethal *Leptospira interrogans* infection. *Infect Immun*. 2015;83(12):4693-4700.
[PUBMED](#) | [CROSSREF](#)
24. Yeh JY, Ga AR. Systemic cytokine response in pigs infected orally with a *Lawsonia intracellularis* isolate of South Korean origin. *J Vet Med Sci*. 2018;80(1):13-19.
[PUBMED](#) | [CROSSREF](#)
25. Pié S, Lallès JP, Blazy F, Laffitte J, Sève B, Oswald IP. Weaning is associated with an upregulation of expression of inflammatory cytokines in the intestine of piglets. *J Nutr*. 2004;134(3):641-647.
[PUBMED](#) | [CROSSREF](#)
26. Vannucci FA, Pusterla N, Mapes SM, Gebhart C. Evidence of host adaptation in *Lawsonia intracellularis* infections. *Vet Res*. 2012;43(1):53.
[PUBMED](#) | [CROSSREF](#)
27. Collins AM, Fell S, Pearson H, Toribio JA. Colonisation and shedding of *Lawsonia intracellularis* in experimentally inoculated rodents and in wild rodents on pig farms. *Vet Microbiol*. 2011;150(3-4):384-388.
[PUBMED](#) | [CROSSREF](#)
28. Guedes RM, Gebhart CJ. Preparation and characterization of polyclonal and monoclonal antibodies against *Lawsonia intracellularis*. *J Vet Diagn Invest*. 2003;15(5):438-446.
[PUBMED](#) | [CROSSREF](#)
29. Fourie KR, Choudhary P, Ng SH, Obradovic M, Brownlie R, Anand SK, et al. Evaluation of immunogenicity and protection mediated by *Lawsonia intracellularis* subunit vaccines. *Vet Immunol Immunopathol*. 2021;237:110256.
[PUBMED](#) | [CROSSREF](#)
30. Fourie KR, Wilson HL. Understanding GroEL and DnaK stress response proteins as antigens for bacterial diseases. *Vaccines (Basel)*. 2020;8(4):773.
[PUBMED](#) | [CROSSREF](#)

31. Pluske JR, Pethick DW, Hopwood DE, Hampson DJ. Nutritional influences on some major enteric bacterial diseases of pig. *Nutr Res Rev.* 2002;15(2):333-371.
[PUBMED](#) | [CROSSREF](#)
32. Quintana-Hayashi MP, Padra M, Padra JT, Benktander J, Lindén SK. Mucus-pathogen interactions in the gastrointestinal tract of farmed animals. *Microorganisms.* 2018;6(2):55.
[PUBMED](#) | [CROSSREF](#)
33. McNamara N, Basbaum C. Signaling networks controlling mucin production in response to Gram-positive and Gram-negative bacteria. *Glycoconj J.* 2001;18(9):715-722.
[PUBMED](#) | [CROSSREF](#)
34. Zeng MY, Cisalpino D, Varadarajan S, Hellman J, Warren HS, Cascalho M, et al. Gut microbiota-induced immunoglobulin G controls systemic infection by symbiotic bacteria and pathogens. *Immunity.* 2016;44(3):647-658.
[PUBMED](#) | [CROSSREF](#)
35. Holyoake PK, Cutler RS, Caple IW, Monckton RP. Enzyme-linked immunosorbent assay for measuring ileal symbiont intracellularis-specific immunoglobulin G response in sera of pigs. *J Clin Microbiol.* 1994;32(8):1980-1985.
[PUBMED](#) | [CROSSREF](#)
36. Shepherd FR, McLaren JE. T cell immunity to bacterial pathogens: mechanisms of immune control and bacterial evasion. *Int J Mol Sci.* 2020;21(17):6144.
[PUBMED](#) | [CROSSREF](#)
37. Cheng HY, Ning MX, Chen DK, Ma WT. Interactions between the gut microbiota and the host innate immune response against pathogens. *Front Immunol.* 2019;10:607.
[PUBMED](#) | [CROSSREF](#)
38. Vannucci FA, Gebhart CJ. Recent advances in understanding the pathogenesis of *Lawsonia intracellularis* infections. *Vet Pathol.* 2014;51(2):465-477.
[PUBMED](#) | [CROSSREF](#)
39. Overbergh L, Giulietti A, Valckx D, Decallonne R, Bouillon R, Mathieu C. The use of real-time reverse transcriptase PCR for the quantification of cytokine gene expression. *J Biomol Tech.* 2003;14(1):33-43.
[PUBMED](#)
40. Wang D, Wang H, Brown J, Daikoku T, Ning W, Shi Q, et al. CXCL1 induced by prostaglandin E2 promotes angiogenesis in colorectal cancer. *J Exp Med.* 2006;203(4):941-951.
[PUBMED](#) | [CROSSREF](#)